

Characterization of a lateritic soil in Chad with a view to its use in eco-construction

Taipabé D.^{1,2*}, Doko K. V.^{1**}, Datchossa T. A.¹, Abdourahmane A. I.³,
Mandela T.⁴, Sanou A.^{3,5}, Gibigaye M.¹

¹University of Abomey-Calavi (UAC) : Laboratoire d'Energétique et de Mécanique Appliquées (LEMA), 01 BP 2009 Cotonou, Benin

²Ecole Nationale Supérieure des Travaux Publics, Laboratoire des Bâtiments et des Travaux Publics, BP 60 N'Djamena, Chad

³Félix Houphouët-Boigny National Polytechnic Institute, Laboratory of Industrial Processes for Environmental Synthesis and New Energies (LAPISEN), BP 1093 Yamoussoukro, Ivory Coast

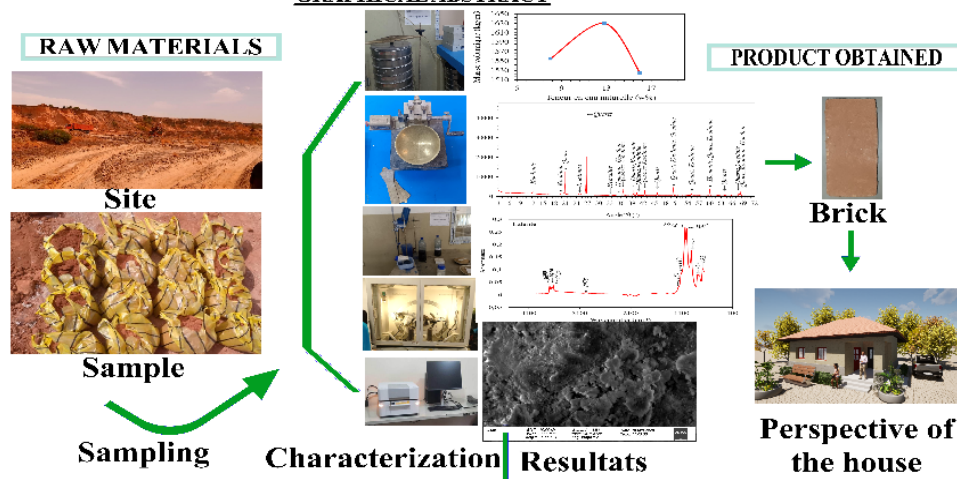
⁴Regional Water & Environmental Sanitation Center Kumasi (RWESCK) Laboratories
Kwame Nkrumah University of Science and Technology (KNUST), Kumasi, Ghana

⁵Higher Normal School, Laboratory of Fundamental and Applied Physical Sciences (LSPFA), 08 BP 10, Abidjan, Ivory Coast

*Corresponding author, Email address: taipabedjouikepouring@gmail.com

**Corresponding author, Email address: dokovalery@yahoo.fr

GRAPHICAL ABSTRACT



Received 17 Apr 2025,
Revised 03 Jun 2025,
Accepted 03 June 2025

Keywords:

- ✓ Lateritic Soil;
- ✓ Characterization;
- ✓ Chad;
- ✓ Valorization;
- ✓ Eco-construction

Citation : Taipabé D., Doko K. V., Datchossa T. A., Abdourahmane A. I., Mandela T., Sanou A., Gibigaye M. (2025). Characterization of a lateritic soil in Chad with a view to its use in eco-construction, *J. Mater. Environ. Sci.*, 16(7), 1189-1209

Abstract: This article focuses on the characterization of a lateritic soil in southern Chad in the city of Moundou. This study led us to study the physical, geotechnical, chemical, mineralogical and microstructural characteristics of this soil. It appears that the natural water content, loss on ignition, gross pH and swelling rate of laterite were obtained with the following respective values: 12.8%, 3.83%, 4.85 and 0.57%. The VBS 1.9 g/100g found, is located in the sandy-clayey soil zone, highlighting the low activity of the clay fraction. X-ray diffraction of this lateritic soil reveals kaolinite, quartz, goethite and hematite as the main constituents. The Calculation of the degree of lateritization of the sample studied gives a value (1.03) lower than 1.33, thus classifying it as a true laterite. The SEM image of the sample allows to see platelets with irregular contours superimposed on each other, typical of Kaolinite and compact surfaces corresponding to quartz. In summary, the characterized lateritic earth has advantages of soil usable for the manufacture of raw bricks. Being an easily accessible material at low cost in the said locality, laterite offers possibilities of use and valorization in the field of eco-construction.

1. Introduction

For several centuries, earth has been one of the most used materials throughout the world, particularly in Sub-Saharan Africa (Alexandre, 2002). Given its accessibility and ease of implementation, earth has remained the material of choice (Issiakou, 2016). It allowed men to provide shelter against bad weather, particularly wind, heat and precipitation. It is these bad weather conditions which directly or indirectly gauge the quality of the earth material used (Fall *et al.*, 2021). Because it must be said, several varieties of earth are available to man for construction. As for our case study, it is laterite. It is a material prized for its physicochemical but also thermomechanical characteristics (Issiakou *et al.*, 2015). Although not the perfect material for sustainable construction, the advantages of laterite have been proven in several African countries. For countries where the weather is rather hot, it is not uncommon to find that in urban areas, the increasing use of so-called energy-intensive and polluting materials such as concrete is redundant (Adadja *et al.*, 2020), (Setiawan *et al.* 2015). However, concrete does not seem to be the thermally suitable material for these types of climates where, during periods of high heat, the temperature easily reaches around 40°C (Herawati *et al.*, 2015).

Laterite is a mass of earth of various colors (pink, ochre, red or brown) very widespread in tropical and equatorial zones but also in some sub-Saharan countries. It is composed of iron oxides such as goethite, limonite, hematite. It also contains aluminum oxides (Gibbsite and Boehmite) and clay minerals (Kaolinite, Halloysite and Illite) (Schellmann, 2003). Laterite is a material that is frequently used in the road sector as well as in buildings (Natural Risks, 2020).

In Chad, specifically in the south of the country (Moundou), it is quite popular for the construction of individual houses. The use of this material is justified not only because of its accessibility and low cost, but also for its performance and physicomaterial properties (Abhilash *et al.*, 2016), (Karka and Djoui, 2019), (Taïpabé *et al.*, 2025). In this case, it is the ecological material par excellence desired. Precisely, the principle of eco-construction would require materials to be easily accessible, recyclable, less energy-intensive and inexpensive. Criteria that this material easily meets. It is therefore necessary to promote this material in this area (Bobet *et al.*, 2020), (Laurent, 1987).

The aim of this study was to investigate the potential use of lateritic soil from Moundou (Chad) as a raw material in eco-construction. To achieve this, the physicochemical and geotechnical properties, including moisture content, loss on ignition, organic matter, density, pH, particle size, methylene blue value, chemical, mineralogical, morphological, microstructural composition, optimal water content, as well as Atterberg limits were determined.

2. Materials and methods

2.1 Presentation of the study area

Recognized as the economic capital of Chad, Moundou is the capital of the province of Logone Occidental and the department of Lac Wey. It is located in the extreme southwest of the country, approximately 470 km south of the capital N'Djamena. The city is divided into four districts and twenty neighborhoods with an estimated population of over 200,000 inhabitants (INSEED, 2024) **Figure 1** shows the study area. Meteorological data, provided by the National Meteorological Agency, are reported in **Figure 2** (ANAM, 2025).

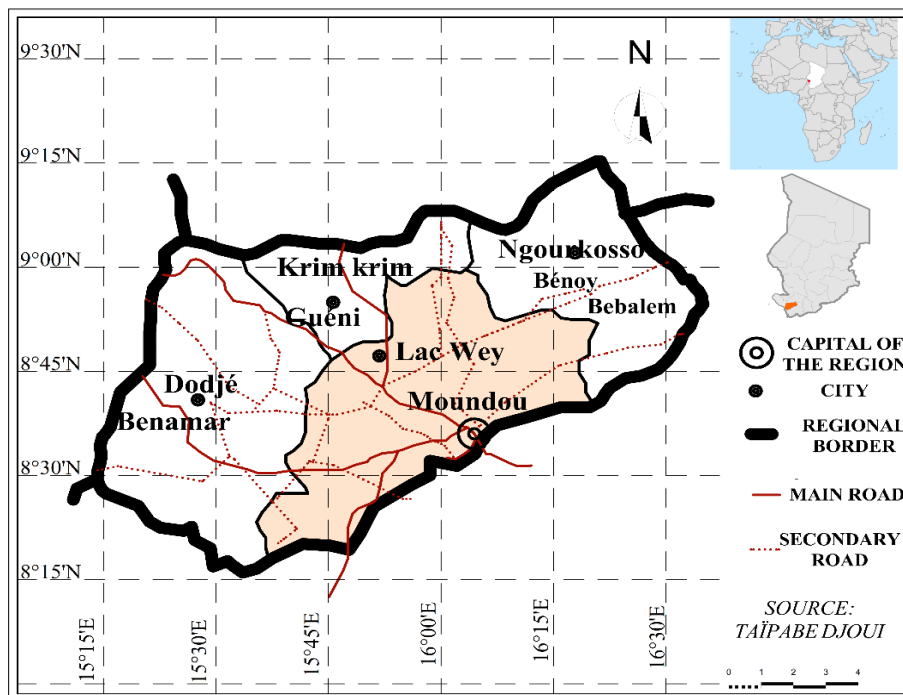


Figure 1. Map of the study area

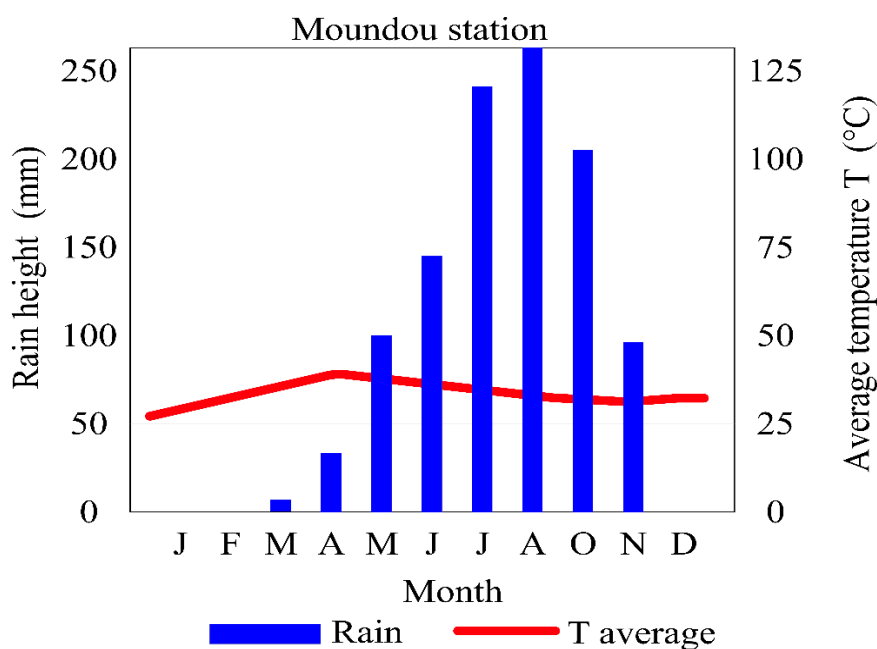


Figure 2. Annual cycle of precipitation and average temperature regime (1981-2022) (Ngaryamngaye et al., 2024)

2.2 Laterite sampling

The sample was extracted from the quarry located in the Koutou district at the northern exit of the city between latitude $8^{\circ}36'5''$ N and longitude $16^{\circ}02'28''$ E. Here it was a shallow sampling, less than one meter. A volume of lateritic soil was taken at random from all over the site (Figure 3(a)). Each volume of soil was mixed before being constituted as a sub-sample; this is a reworked sample. The sampling principle is that suggested by the NF ISO 18400-102 standard (NF ISO 18400-102, 2017). These soils are placed in plastic bags and kept at room temperature until the laboratory (Figure 3(c)). Sampling was done in February, which corresponds to the dry season.



Figure 3. Sampling site (a), Google Earth aerial view (b), Sample taken (c)

2.3 Methods for characterizing laterite

2.3.1. Physical characterization

2.3.1.1. Moisture content

Moisture content (MC) calculated by [Eqn. 1](#) was determined by evaluating the mass loss after drying the raw sample in an oven at 105 °C for 24 hours according to the NF P94-050 standard ([AFNOR, 1995](#)).

$$MC (\%) = \frac{m_1 - m_2}{m_1} \times 100 \quad \text{Eqn. 1}$$

With: m_1 : mass of the soil sample in its natural state (5 g) and m_2 : mass of this soil sample after being placed in an oven at 105 °C for 24 hours.

2.3.1.2. Loss on ignition

The loss on ignition (LOI) was obtained after calcination at 1000 °C for 2 hours in the oven of the sample previously dried in the oven at 105 °C ([Nshimiyimana et al., 2020](#)) using [Eqn. 2](#).

$$LOI (\%) = \frac{(m_2 - m_3)}{m_2} \times 100 \quad \text{Eqn. 2}$$

With: m_2 (g): mass of the sample dried at 105 °C for 24 hours and m_3 (g): mass of the sample calcined at 1000°C for 2 hours in a furnace.

2.3.1.3. Determination of pH

The protocol used is that of the standard ([ISO 10390, 2021](#)). Contact is established between the laterite and the solution by magnetic stirring for one hour and the mixture is left to stand for two hours. Then the pH is measured in the supernatant using a pH meter.

2.3.1.4. Organic matter

The organic matter (OM) content was determined according to the hydrogen peroxide method which consists of an attack with oxygenated water, 10 volumes (H₂O₂, 3%), of the material as described by Laibi et al ([Laibi et al., 2017](#)). The organic matter content is calculated using the formula given by [Eqn. 3](#):

$$OM (\%) = \frac{m_0 - m_1}{m_0} \times 100 \quad \text{Eqn. 3}$$

With: m_0 (g): initial mass of the clay sample before reaction with hydrogen peroxide (100 g) and m_1 (g): mass of the sample after reaction and baked at 105 °C for 24 hours.

2.3.1.5. Swelling rate

The swelling rate TG (%) was determined by the difference in volumes of 20 g of laterite powder initially dried at 105 °C for 24 hours in a 250 mL graduated cylinder (V_1) and that of the same powder after its introduction into another 250 mL graduated cylinder containing 100 mL of distilled water (V_2) according to [Eqn. 4](#). The whole being previously left to stand for 24 hours at room temperature.

$$TG = \frac{(V_2 - V_1)}{V_1} \times 100 \quad \text{Eqn. 4}$$

2.3.1.6. Density

Bulk density (ρ) was determined as the ratio of sample mass to volume (Mierzwa-Hersztek et al., 2019) according to [Eqn. 5](#) (Sanou *et al.*, 2020):

$$\rho = \frac{m_1 - m_0}{V} \quad \text{Eqn. 5}$$

With: ρ : bulk density; m_0 : mass of the graduated cylinder; m_1 : mass of the graduated cylinder containing the sample and V : volume of the graduated cylinder

2.3.2. Geotechnical characterization

2.3.2.1. Granulometric analysis

It allows us to determine and observe the different diameters of the grains that make up laterite by a sieving combination. The procedure used is that which applies to the material retained on a 2 mm mesh sieve. After weighing the sample, it is placed on the sieve 20 mm while sieving it in this way until the next smaller sieve chosen. Each mass of material retained is noted. The proportions in masses retained as well as that passing through the sieves are presented in the form of a table then translated into a curve (ISO 11277, 2020).

2.3.2.2. Proctor test

The Proctor test is intended to determine the optimum water content for a given soil and aims to obtain the relationship between the water content and the dry density of a compacted soil. The standard used is that of (NF P94-093, 2014): Measurement on samples compacted in the Normal Proctor mold – Determination of water content by the Proctor method.

2.3.2.3. Methylene blue test

This test aims to characterize the clayiness of the material. It applies to soils and certain rock materials. It measures the capacity of fine elements to absorb methylene blue. It was carried out according to standard NF P94-068 (AFNOR, 1998). The procedure consists of measuring the quantity of methylene blue absorbed by the 0/5 mm fraction of the material suspended in water. This quantity is related to the 0/50 mm fraction of the material. The value of the blue absorbed by the soil is obtained by [Eqn. 6](#):

$$VBS = \frac{B}{m_s} \times C \times 100 \quad \text{Eqn. 6}$$

VBS (g/100): methylene blue value; B : mass of blue introduced (10 g/L solution); m_s : dry mass of the test sample and C : proportion of 0/5 mm (subject to the test) in the 0/50 mm fraction of the dry material.

2.3.2.4. Atterberg limits

The limits of Atterberg are conventional physical constants (weight water content W) which mark the thresholds between the passage of a soil from the liquid plastic state (liquidity limit LL) and the passage of a soil from the plastic state to the solid state (plasticity limit LP) and make it possible to define indicators qualifying the plasticity of a soil and more precisely to predict the behavior of the soils. These limits were determined by the Casagrande method according to the French standard NF P 94-051 (AFNOR, 1993) at the Laboratory of Building and Public Works (LBTP) in Chad. The liquid limit (LL) and plastic limit (LP) were measured by the Casagrande box method while the plasticity index (PI) was deduced by taking the difference between LL and LP (Eqn. 7):

$$IP = LL - LP \quad \text{Eqn. 7}$$

Clay particle activity is defined as the ratio of the plasticity index to the total clay content (%Clay) in the sample (Nzeukou Nzeugang *et al.*, 2021):

$$A = \frac{IP}{\% \text{ Clay}} \quad \text{Eqn. 8}$$

The coherence index (CI) is derived from the Atterberg limits and indicates the firmness of the soil and changes in water content that allow it to vary between states: liquid, very soft, soft, stiff, very stiff and hard (De Oliveira *et al.*, 2019). The consistency index can be calculated with Eqn. 9 (De Oliveira *et al.*, 2019):

$$IC = \frac{LL - W}{LL - LP} \quad \text{Eqn. 9}$$

The liquidity index (LI) can be calculated as a ratio of the difference between the natural water content, the plastic limit and the liquid limit according to Eqn. 10 (Karakan, 2022).

$$IL = \frac{W - LP}{LL - LP} \quad \text{Eqn. 10}$$

With: W : natural water content.

2.3.3. Chemical characterization

The chemical oxide composition of laterite was determined by X-ray fluorescence (XRF) spectrometry using a PanAlytical Epsilon 4 model energy dispersive X-ray fluorescence (EDXRF) spectrometer.

The results of the percentages of oxides obtained made it possible to characterize the laterite by determining the ratio $\frac{S}{R}$ according to Eqn. 11 (Martin and Doyne, 1927), (Sanou *et al.*, 2020) Eqn. 12 (Maiti *et al.*, 2013), (Persons, 1995).

$$\frac{S}{R} = \frac{\frac{SiO_2}{60}}{\frac{Al_2O_3}{102} + \frac{Fe_2O_3}{160}} \quad \text{Eqn. 11}$$

$$\frac{S}{R} = \frac{SiO_2}{Al_2O_3 + Fe_2O_3} \quad \text{Eqn. 12}$$

With: S : mass percentage of silica and R : percentages of iron and aluminum sesquioxides.

The ratio $\frac{S}{R}$ allows the following classification to be established: $\frac{S}{R} < 1,33$: true laterite ; $1,33 < \frac{S}{R} < 2$: lateritic rock and $\frac{S}{R} > 2$: non-lateritic raw material (Martin and Doyne, 1927).

2.3.4. Mineralogical characterization

2.3.4.1. X-ray diffraction

The mineralogical composition of the laterite powder was determined by powder X-ray diffraction (XRD) using a diffractometer powder X-ray (Panalyan) operating at 45 kV and 40 mA at the X-Techlab Laboratory in Sémé City, Benin. These PXRD analyses were performed using the monochromatic radiation of CuK α radiation ($\lambda = 1.54056$). These phases were identified using HighScore software and a PDF database (powder diffraction files) from the ICDD (International Center for Diffraction Data).

2.3.4.2. Fourier transform infrared spectroscopy

Infrared absorption spectra were obtained with a spectrometer computer-controlled Agilent Cary 630 FTIR Fourier transform scanner, scanning from 4000 to 650 cm⁻¹. FTIR analysis was performed at Laboratory of Chemistry and Renewable Energies (LaCER) of the Nazi BONI University, Bobo-Dioulasso (Burkina Faso).

2.3.4.3. Semi-quantitative analysis

The coupling of chemical analysis and X-ray diffraction made it possible to quantify the percentage of the mineral phases present in the sample using the calculation technique proposed by Yvon et al (Yvon *et al.*, 1982).

$$T(a) = \sum M_i P_i(a) \quad \text{Eqn. 13}$$

T(a): percentage content (%) of oxide "a" in the sample;

M_i: percentage content (%) of mineral "i" in the sample;

P_i(a): proportion of oxide "a" in mineral "i" (this proportion is deduced from the ideal formula attributed to mineral "i").

The approach semi-quantitative was carried out on the basis of the following approximations:

- Fe₂O₃ is distributed between goethite and hematite;
- Al₂O₃ is contained in kaolinite;
- SiO₂ is distributed between kaolinite and quartz.

Based on the approximations given above, the mass percentages of the minerals were obtained from the equations (Eqn. 14, Eqn. 15, Eqn. 16, Eqn. 17):

$$\bullet \quad \% \text{Kaolinite} = \% Al_2O_3 \times \frac{M_{\text{Kaolinite}}}{M_{Al_2O_3}} \quad \text{Eqn. 14}$$

$$\bullet \quad \% \text{Quartz} = \left(\% SiO_2 - \% \text{Kaolinite} \times \frac{2M_{SiO_2}}{M_{\text{Kaolinite}}} \right) \times \frac{M_{\text{Quartz}}}{M_{SiO_2}} \quad \text{Eqn. 15}$$

$$\bullet \quad \% \text{Goethite} = \frac{\% Fe_2O_3 \times M_{\text{Goethite}}}{M_{Fe_2O_3} + M_{\text{Goethite}}} \quad \text{Eqn. 16}$$

$$\bullet \quad \% \text{Hématite} = \% Fe_2O_3 - \% \text{Goethite} \quad \text{Eqn. 17}$$

2.3.5. Morphological and microstructural characterization

Scanning electron microscopy coupled with energy dispersive X-ray spectroscopy (SEM/EDS) was performed using a Zeiss EVO MA 15 electron microscope (Zeiss, Germany) while quantitative elemental information was obtained with Smart EDX analysis (Zeiss, Germany). The analysis was performed at the Kwame Nkrumah University of Science and Technology (Ghana).

3. Results and Discussion

3.1 Physical characteristics

3.1.1. Moisture content

The moisture content is $1.36 \pm 0.03\%$. This value shows that the sample is poorly hydrated by atmospheric water (Bakuan, 2018). This value is close to that reported by Bodian et al. for the Thickly laterite in Senegal which is 1.50% (Bodian et al., 2021).

3.1.2. Loss on ignition

The loss on ignition of laterite is $3.83 \pm 0.04\%$. The value recorded in the present study is much lower than those obtained for laterites from the Cote d'Ivoire (10,16%) (Kouamé et al., 2021) and Burkina Faso ($13.6 \pm 1.5\%$) (Ouedraogo et al., 2020). This low loss on ignition value suggests the presence of a small amount of clay mineral phases in this sample (Kouame, 2021). Indeed, this parameter would be linked to the dehydroxylation of clay minerals, to the oxidation of organic matter and to the decomposition of carbonates and hydroxides present in the sample (Kagonbé et al., 2021).

3.1.3. Organic matter

The laterite studied has an organic matter content of $1.47 \pm 0.12\%$ which is less than 2% ($OM < 2\%$). This value indicates that the laterite is an inorganic soil from a geotechnical point of view (Kouamé et al., 2021). This low value of organic matter in laterite is favorable for good stabilization and durability of the bricks produced (Kouamé et al., 2021). Indeed, the low values of organic matter has a negligible effect in the manufacturing processes (stabilization or cooking) of bricks (Bodian et al., 2021). The value recorded in the present study is very close to that of Thickly laterite (1.46%) already used for making raw earth bricks in Senegal.

3.1.4. Potential hydrogen

The lateritic raw material had a pH equal to 4.85 ± 0.45 . This value indicates that the laterite studied is of a natural acid.

3.1.5. Swelling rate

The swelling rate is an essential property of clay materials, reflecting their swelling or non-swelling character and providing information on the nature of the minerals present in the sample. The swelling rate of laterite is very low ($0.57 \pm 0.13\%$). This low value indicates that the laterite is non-swelling and could be used for making earth bricks for construction.

3.1.6. Bulk density

Bulk density is the mass of a given volume of soil, including the network of pore spaces (Nzeukou Nzeugang et al., 2021). The apparent density of the laterite raw material was 1.25 g/mL. Laterites generally have apparent density values between 1.02 and 2.2 g/mL (Santha Kumar et al., 2022). The sample studied would therefore be a laterite and can be used for the production of bricks (Rimbarngaye et al., 2022).

Comparing the results of the physical characterization of the studied sample with those found in the literature for other lateritic soils used in construction, the results indicate that laterite could be used for construction. However, the geotechnical parameters were also studied.

3.2 Geotechnical characteristics

3.2.1. The Proctor Test

Figure 4 shows the Proctor test curve. The optimum density of soils is an important parameter in determining the quality and durability of earth bricks (Delgado and Guerrero, 2007). The optimum density (δ_{opt}) of laterite is 1630 kg/m^3 . This value is within the recommended range for compressed stabilised soil bricks (1500 to 2000 kg/m^3) (Rimbargaye *et al.*, 2022), (Riza *et al.*, 2010), thus suggesting that the studied laterite can be used for the formulation of stabilized bricks. The Proctor test allowed us to determine the optimal water content (W_{opt}) required to obtain the best compression of the laterite. Indeed, the optimal water content is significant in determining the amount of water that can be added during the production of the earth brick (Kamga Djoumen *et al.*, 2023). In the present study, we recorded a value of 12.8%. This value is higher than those obtained by Taypondou Darman *et al.*, which range between 9.42 and 11.34% (Taypondou Darman *et al.*, 2022) but lower than that reported by Mengue *et al.*, which is 17.80% (Mengue *et al.*, 2017). However, our value is close to that reported by Okonkwo *et al.* (13.85%) for lateritic soils used for making earth bricks (Okonkwo *et al.*, 2022).

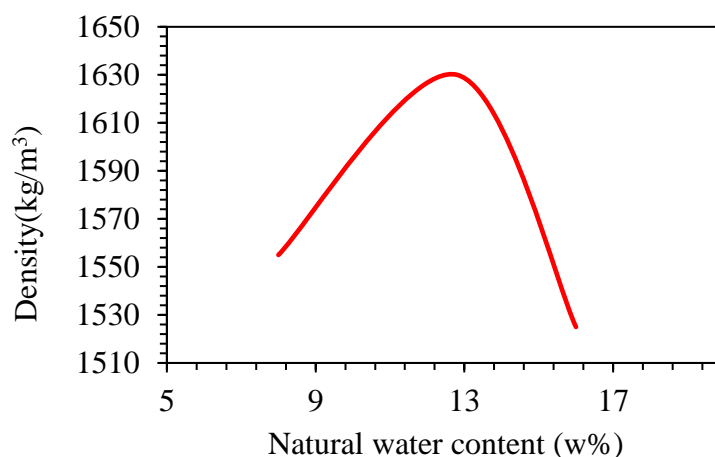


Figure 4. Proctor curve

3.2.2. Granulometric analysis

Soil texture is one of the most important parameters for their use as construction materials. (Delgado and Guerrero, 2007), (Taypondou Darman *et al.*, 2022). Analysis of particle size distribution in the sample shows that sand is the dominant element with 62%. Clay and silt represent 21% and 17% respectively in laterite (Table 1). From these data, laterite can be classified as a sandy-clayey-loamy soil (BSI, 1990) or even like sandy-clay soil (Taypondou Darman *et al.*, 2022). Laterite is mainly made up of sand (62%). This high sand content is an advantage for the use of the sample studied as a raw material for the production of earth bricks. Indeed, the percentage of sand in this soil is within the 60-70% range recommended by Malombe (Malombe, 2015). Furthermore, it has been indicated that the compressive strength of earth bricks increases with a high percentage of sand and a better result is obtained for a proportion of sand between 40 and 65% (Guettala *et al.*, 2002), (Kwon *et al.*, 2010), (Taypondou Darman *et al.*, 2022). In addition, a certain high proportion of coarse grains is necessary because they constitute the skeleton of the earth brick and ensure the stability of its structure

(Taypondou Darman *et al.*, 2022). Laterite is made up of 21% clay. This proportion of clay in the material is a favorable asset for its use as a construction material. Indeed, a content of between 5% and 30% clay gives laterite good cohesion in its natural state (Kouakou *et al.*, 2022) because the clay in the material acts as a natural cement, tending to bind the soil particles and thus improve the mechanical characteristics of the earth brick (Taypondou Darman *et al.*, 2022). In addition, authors have indicated that soils with a clay content between 15 and 30% are suitable for the production of earth bricks (Kwon *et al.*, 2010).

Table 1. Particle size distribution

Particles	Sand (> 80 µm)	Silt (2 - 80 µm)	Clay (< 2 µm)
Percentage	62%	17%	21%

3.2.3. Plastic properties

The plastic properties of the material were determined from the Atterberg limits. The results are recorded in the **Table 2**. The liquid limit of the studied laterite is 39%. It has been recommended that a good soil for stabilizing earth blocks has a liquid limit of less than 40% (LL < 40%). Indeed, a soil with a LL greater than 40% (LL > 40%) results in low compressive strength (Burroughs, 2008). Since the liquid limit of laterite is less than 40%, it can be used for the production of earth bricks.

The plastic limit of the sample studied is 22.08%. The higher the plastic limit, the more clayey the soil. This could therefore explain the sandy-clayey nature of the soil studied. Soils with plastic limits between 16 and 19% are favorable for the stabilization of earth blocks (Burroughs, 2008). The value recorded in the present study is higher than the maximum value of the interval. This could induce high values of the withdrawal limit (Rimbarngaye *et al.*, 2022).

Table 2 shows that the plasticity index (PI) of laterite is 16.92%. The sample studied is therefore plastic because the plasticity value is included in the plastic domain which is $15 \leq IP \leq 45$ (Boussen *et al.*, 2016). In addition, the plasticity index of the soil is less than 25%. According to Burroughs, a good soil for stabilization should have a plasticity index less than 25% (Burroughs, 2008). In addition, soils with a plasticity index greater than 20% are not suitable for manual compaction (Walker, 1995). Such a soil develops much more shrinkage and the compressive strength is low (Rimbarngaye *et al.*, 2022). The consistency index (CI) has a value of 1.55; thus, suggesting that the material has a plastic character. In addition, the liquidity index (LI) with a value of -0.57 is less than zero (LI < 0). This value gives the material a hard plastic consistency character (Bishweka *et al.*, 2021), (Kamga Djoumen *et al.*, 2023). The plastic properties thus studied indicate that the lateritic soil is of good quality and can be used for the production of blocks.

Table 2. Plastic characteristics of laterite

Plastic properties	Values
Liquidity Limit (LL)	39%
Plasticity Limit (PL)	22.08%
Plasticity Index (PI)	16.92%
Consistency Index (CI)	1.55
Liquidity Index (LI)	- 0.57

3.2.4. Methylene blue value and activity of clay particles

The value of methylene blue (VBS) to characterize the clay content of a soil is 1.9 g/100 g for laterite. This value shows that the material studied is a soil sandy-clayey, not very plastic because included in the domain $1.5 \leq \text{VBS} \leq 2.5$ (Sanou, 2017). Furthermore, the relatively low VBS value highlights the low activity of the clay fraction and suggests an absence of swelling clay minerals (Kouamé *et al.*, 2021) such as smectite (montmorillonite) in the sample. These results are consistent with those of the particle size analysis and those of the Atterberg limits with regard to the nature of the soil.

Soil activity (A), indicating the physical and mechanical activity of the clay fraction, was determined. The obtained value is 0.8. According to Skempton's classification based on the activity of fine particles, the sample studied has normal activity ($0.75 < A < 1.5$) (Penka *et al.*, 2022). Activity depends primarily on the dominant clay minerals, cations, and exchangeable salts in the soil solution (Zolfaghari *et al.*, 2015). The normal activity of the sample is probably due to the presence of kaolinite which is less active (0.4) (Penka *et al.*, 2022). This activity against methylene blue can be extended to other dyes or heavy metals as found in literature (Jaber Ibrahim *et al.*, 2023), (Aaddouz *et al.*, 2022; Akartasse *et al.*, 2022), (Azzaoui *et al.*, 2019).

3.3 Mineralogical and chemical characteristics

3.3.1. X-ray diffraction

The X-ray diffraction results of the sample are given in Figure 5. The diffractogram analysis indicates that the soil sample studied consists mainly of kaolinite, quartz, goethite and hematite. These minerals are the main minerals generally identified in laterites (Kouamé *et al.*, 2020), (Santha Kumar *et al.*, 2022). Indeed, laterites are generally composed of secondary minerals of aluminum, quartz and kaolinite (Rimbarngaye *et al.*, 2022). The absence of 2/1 type clay minerals (smectite) on the diffractogram confirms the results of the physical and geotechnical characterization. This absence of smectite-type minerals is an advantage for the use of the sample as a construction material. Indeed, the presence of clay minerals such as smectites in materials used for geotechnical purposes influences their properties, in particular their water absorption and swelling (Logmo *et al.*, 2013).

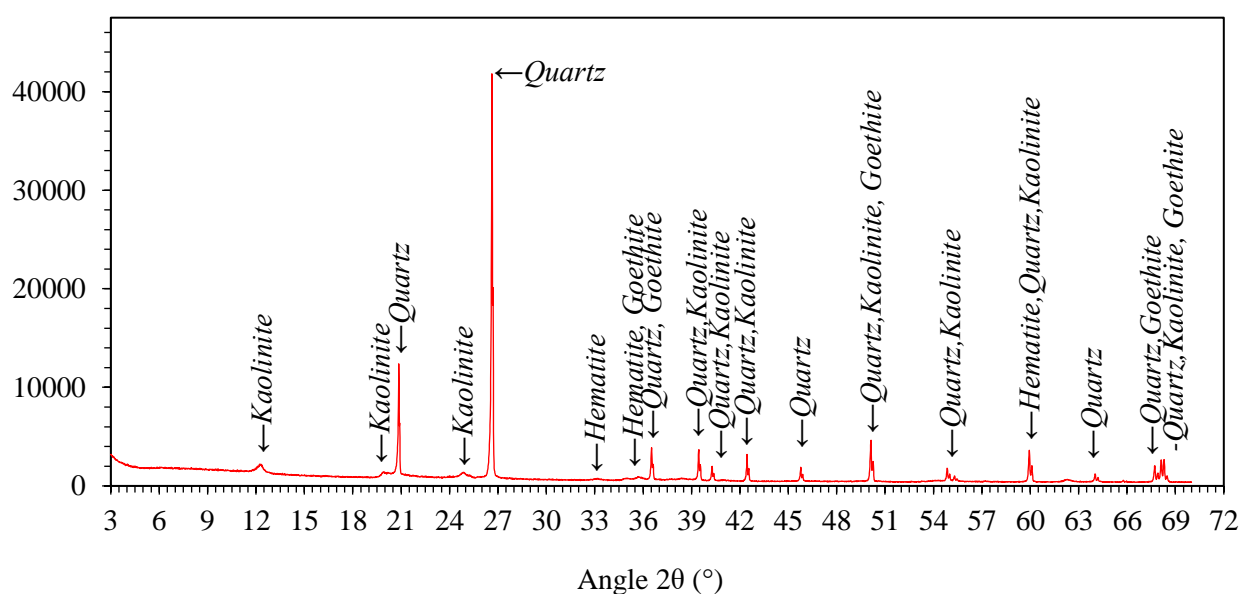


Figure 5. XRD of laterite

3.3.2. Chemical composition

The chemical composition of laterite in terms of oxides determined by XRF is presented in **Table 3**. It is found that laterite is composed mainly of SiO₂, Al₂O₃ and Fe₂O₃, with high percentages. These compounds represent 82.01% of the total oxide composition. In addition, minor components, such as K₂O, MnO, TiO₂ and Na₂O were also present in laterite (**Table 3**). This observation has also been reported by other researchers when they performed XRF analysis of laterites (*Abdullah et al., 2017*), (*Bodian et al., 2018*), (*Djinsi Vaimata et al., 2024*), (*Ouedraogo et al., 2020*).

Table 3. Percentage of oxides in laterite

Chemical composition in oxides								
Oxides	H ₂ O	SiO ₂	Al ₂ O ₃	Fe ₂ O ₃	K ₂ O	Na ₂ O	TiO ₂	MnO
%	12.35	41.57	29.12	11.32	2.37	0.76	1.39	0.14

3.3.3. Degree of lateritization

The degree of lateritization is defined as the silica-sesquioxide ratio (S/R). The S/R ratios for the sample in the present study are calculated using the chemical composition obtained from the XRF results. The value of the S/R ratio is equal to 1.94 and is between $1.33 < S/R = 1.94 < 2$ (**Eqn. 9**), which indicates that the sample studied would be a lateritic rock (*Martin and Doyne, 1927*). However, the S/R ratio value calculated from **Eqn. 10** is 1.03 and is less than 1.33 ($S/R = 1.03 < 1.33$), thus suggesting that the collected sample is a true laterite (*Maiti et al., 2013*). However, according to both approaches, the sample studied is a laterite soil.

3.3.4. Semi-quantitative analysis

The coupling of chemical analysis and mineralogy through the relationship of Yvon et al (*Yvon et al., 1982*) allowed to determine the percentage of mineral phases in the sample. **Table 4** represents the results of the semi-quantitative analysis. These results show that the sample is composed of hematite (7.27%), goethite (4.05%), kaolinite (73.66%) and quartz (7.31%). Goethite and hematite represent 11.32% of the minerals present in the sample. The characteristic red color appears from iron compounds present in laterite (*Maiti et al., 2013*). Furthermore, kaolinite is the only clay mineral present in the sample. This mineral is well known for its low water absorption capacity and its prevalence in materials used for the production of earth bricks increases the molding properties (*Kamga Djoumen et al., 2023*).

Table 4. Mineralogical composition (%) of laterite

Minerals	Goethite	Hematite	Kaolinite	Quartz	Total
% by mass	4.05	7.27	73.66	7.31	92.29

3.3.5. Infrared spectroscopy

Figure 6 shows the infrared spectrum of the laterite sample, recorded in the frequency range 4000-650 cm⁻¹. The spectrum presents the vibration bands generally observed in lateritic materials. The assignments of the characteristic bands of the functional groups in the infrared spectrum were made based on the data provided in the literature. The bands observed around 3690, 3649 and 3622 cm⁻¹ correspond to the vibration bands of the OH groups of kaolinite (*Gauly et al., 2025*), (*Meite et al., 2018*). The bands around 3690 and 3649 cm⁻¹ are attributed to the vibrations of the external hydroxyls of kaolinite and that around 3622 cm⁻¹ corresponds to the vibrations of the internal hydroxyls

(Madejová and Komadel, 2001). These bands have also been attributed to other hydroxylated compounds in laterites, including goethite (Djinsi Vaïmata *et al.*, 2024). The absence of a well-defined peak around 3669 cm^{-1} suggests that the kaolinite present in the sample has a disordered structure (Matusik *et al.*, 2012). The absorption band observed around 1630 cm^{-1} is attributed to the hydration water of laterite (Djinsi Vaïmata *et al.*, 2024). The absorption bands observed around 1110 cm^{-1} and 1002 cm^{-1} are due to the stretching vibrations of the Si-O bonds of kaolinite (Madejová and Komadel, 2001), (Sanou *et al.*, 2024). The infrared spectrum shows the band associated with the vibrations of the elongation of the Si-O-Si bond of kaolinite around 1032 cm^{-1} (Kouamé *et al.*, 2021). This band has also been attributed to the Fe-OH bond of goethite (Ristić *et al.*, 2006). The band around 909 cm^{-1} is attributable to the deformation vibrations of the Al-OH bonds of kaolinite (Ouedraogo *et al.*, 2020). This band is also attributed to Fe-O stretching, indicating the presence of hematite in the laterite (Eisazadeh *et al.*, 2011). The band at 767 cm^{-1} can be attributed to the Si-O-Al bonds of kaolinite (Kouamé *et al.*, 2021). This band to 767 cm^{-1} is also attributable to bending vibrations of the Fe-OH bond (Sanou *et al.*, 2020). The spectrum also shows the presence of quartz vibration band which is observed at 682 cm^{-1} , characteristic of Si-O-Si bonds (Kouamé *et al.*, 2021). According to literature, the band around 682 cm^{-1} is attributable to Fe-OH vibrations and associated with the kaolinite-hematite composite (Ioannou and Dimirkou, 1997), (Maiti *et al.*, 2013).

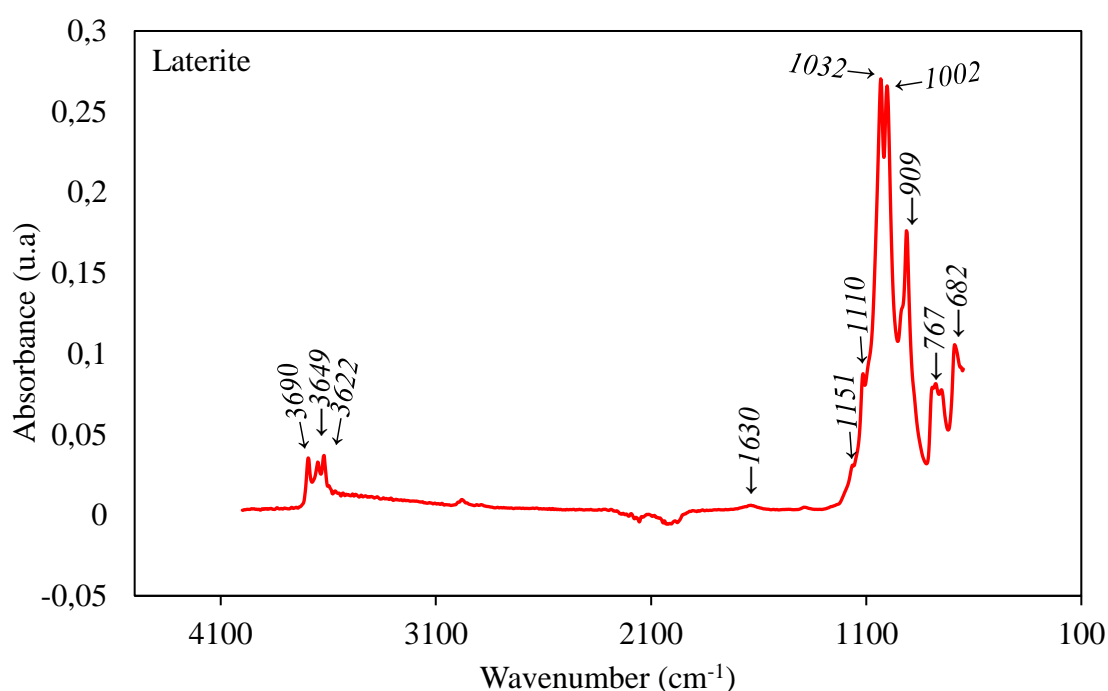


Figure 6. Infrared spectroscopy

3.4 Morphological and microstructural characteristics

Figure 7 presents the morphology of the laterite sample. Observation of the SEM image shows platelets (sheets) with irregular contours similar to kaolinite particles. Indeed, several researchers have characterized nanoscale kaolinite particles as having a quasi-hexagonal lamellar structure (Caillère *et al.*, 1982), (Suzuki *et al.*, 2013). These same observations have been made by other authors on clayey materials containing kaolinite (Fort *et al.*, 2024), (Gauly *et al.*, 2025), (Sanou *et al.*, 2024), (Soro *et al.*, 2023). In addition, these platelets are stacked on top of each other to form clusters. This morphology is similar to that generally observed in poorly crystallized kaolinites (Kouamé *et al.*, 2021).

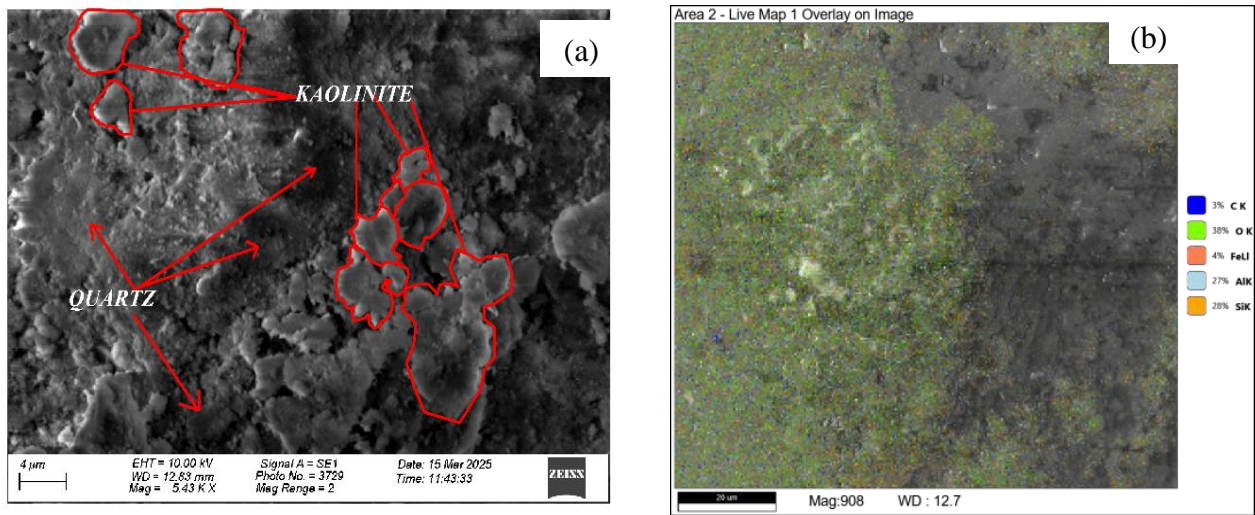


Figure 7. SEM image of the sample (a), sample mapping (b)

Quantitative elemental analysis indicates the presence of certain elements and their mass percentages in the sample (Figure 8 and Table 5). The presence of the elements Si, Al, O, Fe and C is noted. The elements Si and Al are respectively the major constituents of the octahedral and tetrahedral sites of the kaolinite sheets (Bouna *et al.*, 2020). The presence of Fe in the sample confirms the presence of goethite and hematite in the sample. These results are consistent with the chemical composition and mineralogy of the sample.

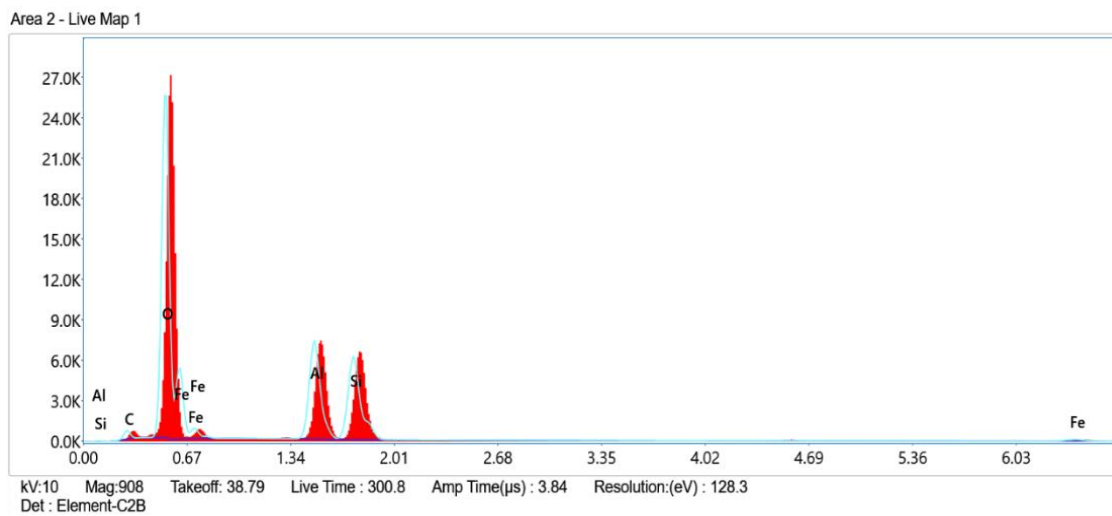


Figure 8. EDS spectrum of laterite

Table 5. Quantitative of constituents

	Chemical elements				
	C	O	Al	Fe	Si
Weight	8.07	58.47	15.12	14.57	3.77
Percentage	12.28	66.77	10.24	9.48	1.23

Conclusion

The purpose of this study was to characterize the lateritic soil of Chad with a view to its use in the eco-construction of individual houses. The study showed that:

- The laterite studied consists mainly of kaolinite, quartz, goethite and hematite;
- Its physical characterization showed that its humidity rate is $1.36\pm 0.03\%$, its loss on ignition is $3.83\pm 0.04\%$, its organic matter rate is $1.47\pm 0.12\%$ for a pH equal to 4.85 ± 0.45 ;
- It is non-swelling;
- Its chemical composition mainly includes oxides of SiO_2 , Al_2O_3 and Fe_2O_3 , with high percentages.
- Microscopic observation confirms the presence of irregularly shaped, poorly crystallized kaolinite and quartz.

In view of these characteristics and the values obtained after study, this lateritic earth is not only suitable for the construction of houses, but specifically for the production of blocks, in this case adobe bricks.

Author credit: contribution statement: Taïpabé Djoui: Writing - revision, Writing - original version, Methodology, Investigation. Valéry Kouandété Doko: Writing, Methodology, Investigation., Tiambo Abbas Datchossa: Writing, Methodology, Investigation., Ali Sanou: Writing of the original draft, Methodology, Adamou Ibro Abdourahamane: Methodology, Investigation., Mandela Toku: Methodology, Investigation., Mohamed Gbigaye: Writing, Methodology.

Acknowledgement: Authors would like to thank all the technicians at the “Laboratoire d’Énergétique et de Mécanique Appliquées” (LEMA) at the Université d’Abomey-Calavi (UAC) Benin, and those at the “X-TECHLAB”, Sémé City, Benin, for their constant help in carrying out the tests.

Disclosure statement: *Conflict of Interest:* The authors declare that there are no conflicts of interest. *Compliance with Ethical Standards:* This article does not contain any studies involving human or animal subjects.

References

- Aaddouz M., Azzaoui K., Akartasse N., Mejdoubi E., Hammouti B., Taleb M., Sabbahi R., Alshahateet S.F. (2023). Removal of Methylene Blue from aqueous solution by adsorption onto hydroxyapatite nanoparticles, *Journal of Molecular Structure*, 1288, 135807. <https://doi.org/10.1016/j.molstruc.2023.135807>
- Abdullah, AH, Nagapan, S., Antonyova, A., Rasiah, K., Yunus, R., Sohu, S., 2017. Comparison of Strength Between Laterite Soil and Clay Compressed Stabilized Earth Bricks (CSEBs). *MATEC Web Conf.* 103, 01029. <https://doi.org/10.1051/mateconf/201710301029>
- Abhilash, H., McGregor, F., Millogo, Y., Fabbri, A., Séré, A., Aubert, J.-E., Morel, J.-C., 2016. Physical, mechanical and hygrothermal properties of lateritic building stones (LBS) from Burkina Faso. *Construction and Building Materials* 125, 731–741.
- Adadja, CE, Houngan, CA, Koutsawa, Y., Khelil, A., Vianou, A., Gbaguidi, V., Zahrouni, H., Gbigaye, M., Hattab, M., 2020. Multi-scale modeling of the elastic properties of the clay-rice straw composite.
- AFNOR, 1995. Soils: reconnaissance and testing - Determination of the water content by weight of materials - Steaming method (National standards and national normative documents No. NF P94-050). French Association for Standardization, France.

- AFNOR, 1993. NF P 94-051, Soils: Investigation and Testing - Determination of Atterberg Limits. Cup Liquidity Limit - Roller Plasticity Limit (French Standard No. NF P 94-051). French Association for Standardization, Paris (France).
- Akartasse N., Azzaoui K., Mejdoubi E., Hammouti B., *et al.* (2022), Environmental-Friendly Adsorbent Composite Based on Hydroxyapatite/Hydroxypropyl Methyl-Cellulose for Removal of Cationic Dyes from an Aqueous Solution, *Polymers*, 14(11), 2147. <https://doi.org/10.3390/polym14112147>
- Alexandre, J., 2002. Lateritic cuirasses and other tropical ferruginous formations: example of southern Haut Katanga. *Annalen. Geologische Wetenschappen* 107.
- ANAM, 2025. The climate of our cities meteo Chad [WWW Document]. URL. <https://www.meteochad.org/le-climat-de-nos-villes/> (accessed 1.8.25).
- Azzaoui K., Mejdoubi E., Lamhamdi A., Lakrat M., Hamed O., Jodeh S., *et al.* (2019) Preparation of hydroxyapatite biobased microcomposite film for selective removal of toxic dyes from wastewater, *Desalination and Water Treatment*, 149, 194-208
- Bakouan, C., 2018. Characterization of some lateritic sites in Burkina Faso: application to the elimination of arsenic (III) and (V) in groundwater (Doctoral Thesis). University of Ouagadougou I Pr JKZ and University of Mons, Burkina Faso/France.
- Bishweka, C., Manjia, MB, Ngague, F., Nana, UJMP, Pettang, C., 2021. Contribution to the Characterization of Lateritic Soils for the Manufacture of Compressed Stabilized Earth Bricks. *OJCE*, 11, 411–426. <https://doi.org/10.4236/ojce.2021.114024>
- Bobet, O., Seynou, M., Zerbo, L., Bamogo, H., Sanou, I., Sawadogo, M., 2020. Mechanical, hydric and thermal properties of raw earth bricks amended with peanut shells. *Journal of the West African Chemical Society* 49, 54–64.
- Bodian, S., Faye, M., Sambou, V., Séne, NA, Diaw, I., Faye, K., 2021. Physicochemical characterization of clay raw materials from the Thick quarry (Senegal) for the manufacture of earth bricks. *JPSOAPHYS* 3, 1–7. <https://doi.org/10.46411/jpsoaphys.2021.01.01>
- Bodian, S., Faye, M., Sene, NA, Sambou, V., Limam, O., Thiam, A., 2018. Thermo-mechanical behavior of unfired bricks and fired bricks made from a mixture of clay soil and laterite. *Journal of Building Engineering*, 18, 172–179. <https://doi.org/10.1016/j.jobee.2018.03.014>
- Bouna, L., El Fakir, AA, Benlhachemi, A., Draoui, K., Villain, S., Guinneton, F., 2020. Physico-chemical characterization of clays from Assa-Zag for valorization in cationic dye methylene blue adsorption. *Materials Today: Proceedings*, 22, 22–27. <https://doi.org/10.1016/j.matpr.2019.08.059>
- Boussen, S., Sghaier, D., Chaabani, F., Jamoussi, B., Bennour, A., 2016. Characteristics and industrial application of the Lower Cretaceous clay deposits (Bouhedma Formation), Southeast Tunisia: Potential use for the manufacturing of ceramic tiles and bricks. *Applied Clay Science*, 123, 210–221. <https://doi.org/10.1016/j.clay.2016.01.027>
- BSI, 1990. Methods of Test for Soils for Civil Engineering Purposes. Compressibility, Permeability and Durability Tests, BS (Series). BSI Standards, London, UK.
- Burroughs, S., 2008. Soil Property Criteria for Rammed Earth Stabilization. *J. Mater. Civ. Eng.* 20, 264–273. [https://doi.org/10.1061/\(ASCE\)0899-1561\(2008\)20:3\(264\)](https://doi.org/10.1061/(ASCE)0899-1561(2008)20:3(264))

- Caillère, S., Hénin, S., Rautureau, M., 1982. Classification and nomenclature, in: *Mineralogy of clays*. Masson, France, p. 189.
- De Oliveira, DGG, Thewes, M., Diederichs, MS, Langmaack, L., 2019. Consistency Index and Its Correlation with EPB Excavation of Mixed Clay–Sand Soils. *Geotech Geol Eng* 37, 327–345. <https://doi.org/10.1007/s10706-018-0612-x>
- Delgado, MCJ, Guerrero, IC, 2007. The selection of soils for unstabilized earth buildings: A normative review. *Construction and Building Materials* 21, 237–251. <https://doi.org/10.1016/j.conbuildmat.2005.08.006>
- Djinsi Vaïmata, G., Djakba, R., Dobe, N., MadiBalo, A., Kaze, RC, Boughzala, H., Massaï, H., 2024. The effect of combining rice husk ash with laterite-based inorganic polymers activated by potassium-rich shea pellet ash. *Sustainable Chemistry and Pharmacy*, 39, 101607. <https://doi.org/10.1016/j.scp.2024.101607>
- Eisazadeh, A., Kassim, KA, Nur, H., 2011. Characterization of phosphoric acid- and lime-stabilized tropical lateritic clay. *Environ Earth Sci* 63, 1057–1066. <https://doi.org/10.1007/s12665-010-0781-2>
- Fall, M., Sarr, D., Cissé, EM, Konaté, D., 2021. Physico-Mechanical Characterization of Clay and Laterite Bricks Stabilized or Not with Cement. *Open Journal of Civil Engineering*, 11, 60–69. <https://doi.org/10.4236/ojce.2021.111004>
- Fort, CI, Sanou, A., Coulibaly, M., Yao, KB, Turdean, GL, 2024. Green modified electrode for sensitive simultaneous heavy metal ions electro detection. *Sensors and Actuators B: Chemical* 418, 136326. <https://doi.org/10.1016/j.snb.2024.136326>
- Gauly, LP, Coulibaly, M., Soro, SB, Kouadio, KS, N'Dri, SR, Sanou, A., Trokourey, A., 2025. Characterization and enhanced performance of Ivorian clays as potential modifiers in carbon paste electrodes. *Discov Appl Sci* 7, 128. <https://doi.org/10.1007/s42452-024-06457-1>
- Guetlala, A., Houari, H., Mezghiche, B., Chebili, R., 2002. Durability of lime stabilized earth blocks. *Courrier du Savoir* 2, 61–66.
- Herawati, H., Suripin, Suharyanto, 2015. Impact of Climate Change on Streamflow in the Tropical Lowland of Kapuas River, West Borneo, Indonesia. *Procedia Engineering* 125, 185–192. <https://doi.org/10.1016/j.proeng.2015.11.027>
- INSEED, 2024. Monthly Bulletin of the National Harmonized Consumer Price Index (INHPC) Chad-August 2024 [WWW Document]. <https://www.inseed.td/index.php/component/jdownloads/category/7-documents-et-publications-demographique?Itemid=-1> (accessed 1.2.25).
- Ioannou, A., Dimirkou, A., 1997. Phosphate Adsorption on Hematite, Kaolinite, and Kaolinite–Hematite (k–h) Systems As Described by a Constant Capacitance Model. *Journal of Colloid and Interface Science* 192, 119–128. <https://doi.org/10.1006/jcis.1997.4970>
- ISO 10390, 2021. Soil, treated biowaste and sludge – Determination of pH.
- ISO 11277, 2020. Soil quality — Determination of particle size distribution in mineral soil material — Method by sieving and sedimentation.
- Issiakou, MS, 2016. Characterization and valorization of lateritic materials used in road construction in Niger.

- Issiakou, MS, Saiyouri, N., Anguy, Y., Gaborieau, C., Fabre, R., 2015. STUDY OF LATERITIC MATERIALS USED IN ROAD CONSTRUCTION IN NIGER: IMPROVEMENT METHOD. Presented at the Rencontres Universitaires de Génie Civil.
- Jaber Ibrahim, A., Abdul Wahid Dwesh, H., R.Y. Al-Sawad, A. (2023) Adsorption of methylene blue dye onto bentonite clay: Characterization, adsorption isotherms, and thermodynamics study by using UV-Vis technique. *Analytical Methods in Environmental Chemistry Journal*, 6(3), 5-18. <https://doi.org/10.24200/amecj.v6.i03.243>
- Kagonbé, BP, Tsozué, D., Nzeukou, AN, Ngos, S., 2021. Mineralogical, physico-chemical and ceramic properties of clay materials from Sekandé and Gashiga (North, Cameroon) and their suitability in earthenware production. *Heliyon* 7, e07608. <https://doi.org/10.1016/j.heliyon.2021.e07608>
- Kamga Djoumen, T., Tiomo, IF, Vouffo, M., Ngapgue, F., Sali, M., Keubou, VWT, 2023. Characterization of basaltic rock laterites in Dschang, West-Cameroon: Compressed Earth Bricks (CEB) for low-cost buildings. *Case Studies in Construction Materials* 19, e02335. <https://doi.org/10.1016/j.cscm.2023.e02335>
- Karakan, E., 2022. Comparative Analysis of Atterberg Limits, Liquidity Index, Flow Index and Undrained Shear Strength Behavior in Binary Clay Mixtures. *Applied Sciences* 12, 8616. <https://doi.org/10.3390/app12178616>
- Karka, BR, Djoui, T., 2019. Earthen habitat construction model: Case of manual adobe in sub-Saharan Africa. *International Journal of Innovation and Applied Studies*, 26, 883–887.
- Kouakou, LPM-S., Kouamé, AN, Doubi, BIHG, Méité, N., Kangah, JT, Zokou, EP, Konan, LK, Andji-Yapi, YJ, 2022. Characterization of Two Clay Raw Materials from Côte d'Ivoire with a View to Enhancing Them in Eco-Construction. *JMMCE*, 10, 198–208. <https://doi.org/10.4236/jmmce.2022.102016>
- Kouamé, AN, Konan, KL, Doubi, GBIH, 2021. Microstructure and Mineralogy of Compressed Earth Bricks Incorporating Shea Butter Wastes Stabilized with Cement. *AM* 10, 67. <https://doi.org/10.11648/j.am.20211004.13>
- Kouamé, AN, Konan, LK, Tognonvi, MT, Oyetola, S., 2020. Mechanical and Microstructural Properties of Compressed Earth Bricks (CEB) Incorporating Shea Butter Wastes and Stabilized with Cement. *Journal of Materials Physics and Chemistry* 8, 1–8.
- Kouame, NA, 2021. Stabilization, by cement, of clayey earth blocks incorporating shea cakes (Doctoral Thesis). Felix Houphouët Boigny University, Abidjan (Ivory Coast).
- Kwon, H.-M., Le, AT, Nguyen, NT, 2010. Influence of soil grading on properties of compressed cement-soil. *KSCE Journal of Civil Engineering* 14, 845–853. <https://doi.org/10.1007/s12205-010-0648-9>
- Laibi, AB, Gomina, M., Sorgho, B., Sagbo, E., Blanchart, P., Boutouil, M., Sohounhloule, DKC, 2017. Physicochemical and geotechnical characterization of two clayey sites in Benin with a view to their development in eco-construction. *Int. J. Bio. Chem. Sci* 11, 499. <https://doi.org/10.4314/ijbcs.v11i1.40>
- Laurent, J.-P., 1987. Thermal properties of earth material. CSTB Notebooks 279, 2156.
- Logmo, EO, Ngon, GFN, Samba, W., Mbog, MB, Etame, J., 2013. Geotechnical, Mineralogical and Chemical Characterization of the Missole II Clayey Materials of Douala Sub-Basin (Cameroon) for Construction Materials. *OJCE* 03, 46–53. <https://doi.org/10.4236/ojce.2013.32A006>

- Madejová, J., Komadel, P., 2001. Baseline Studies of the Clay Minerals Society Source Clays: Infrared Methods. *Clays and Clay Minerals* 49, 410–432. <https://doi.org/10.1346/CCMN.2001.0490508>
- Maiti, A., Thakur, BK, Basu, JK, De, S., 2013. Comparison of treated laterite as arsenic adsorbent from different locations and performance of best filter under field conditions. *Journal of Hazardous Materials* 262, 1176–1186. <https://doi.org/10.1016/j.jhazmat.2012.06.036>
- Malombe, E., 2015. Production of compressed stabilized soil blocks (SSB). Mzuzu University, Department of Land Management, 1–11.
- Martin, FJ, Doyne, HC, 1927. Laterite and lateritic soils in Sierra Leone. *J. Agric. Sci.* 17, 530–547. <https://doi.org/10.1017/S0021859600018815>
- Matusik, J., Gawel, A., Bahranowski, K., 2012. Grafting of methanol in dickite and intercalation of hexylamine. *Applied Clay Science* 56, 63–67. <https://doi.org/10.1016/j.clay.2011.11.023>
- Meite, N., Konan, LK, Bamba, D., Goure-Doubi, BIH, Oyetola, S., 2018. Structural and Thermomechanical Study of Plastic Films Made from Cassava-Starch Reinforced with Kaolin and Metakaolin. *MSA* 09, 41–54. <https://doi.org/10.4236/msa.2018.91003>
- Mengue, E., Mroueh, H., Lancelot, L., Medjo Eko, R., 2017. Physicochemical and consolidation properties of compacted lateritic soil treated with cement. *Soils and Foundations* 57, 60–79. <https://doi.org/10.1016/j.sandf.2017.01.005>
- Mierzwa-Hersztek, M., Gondek, K., Jewiarz, M., Dziedzic, K., 2019. Assessment of energy parameters of biomass and biochars, leachability of heavy metals and phytotoxicity of their ashes. *J Mater Cycles Waste Management* 21, 786–800. <https://doi.org/10.1007/s10163-019-00832-6>
- NF ISO 18400-102 [WWW Document], 2017. Afnor EDITIONS. <https://www.boutique.afnor.org/fr/norme/nf-iso-18400102/qualite-du-sol-echantillonnage-partie-102-choix-et-application-des-techniqu/fa180496/79926> (accessed 3.14.25).
- Ngaryamngaye, S., Djourdebbe, FB, Miambaye, M., 2024. Climate change: searching for signals in Chad through the study of the cities of Bol, Fianga, Moundou and N'Djamena. *ESI Preprints* 20, 82–82.
- Nshimiyimana, P., Fagel, N., Messan, A., Wetshondo, DO, Courard, L., 2020. Physico-chemical and mineralogical characterization of clay materials suitable for production of stabilized compressed earth blocks. *Construction and Building Materials* 241, 118097. <https://doi.org/10.1016/j.conbuildmat.2020.118097>
- Nzeukou Nzeugang, A., Tsozué, D., Kagonbé Pagna, B., Balo Madi, A., Fankam Deumeni, A., Ngos, S., Nkoumbou, C., Fagel, N., 2021. Clayey soils from Boulgou (North Cameroon): geotechnical, mineralogical, chemical characteristics and properties of their fired products. *SN Appl. Sci.* 3, 551. <https://doi.org/10.1007/s42452-021-04541-4>
- Okonkwo, VO, Omaliko, IK, Ezema, NM, 2022. Stabilization of Lateritic Soil with Portland Cement and Sand for Road Pavement. *Open Access Library Journal* 9, 1–15. <https://doi.org/10.4236/oalib.1108560>
- Ouedraogo, RD, Bakouan, C., Sorgho, B., Guel, B., Bonou, LD, 2020. Characterization of a natural laterite from Burkina Faso for the removal of arsenic (III) and arsenic (V) in groundwater. *Int. J. Bio. Chem. Sci* 13, 2959. <https://doi.org/10.4314/ijbcs.v13i6.41>

- Penka, JB, Nana, UJMP, Manjia, MB, Bomeni, IY, Pettang, C., 2022. Hydrological, mineralogical and geotechnical characterization of soils from Douala (coastal, Cameroon): potential used in road construction. *Heliyon* 8, e11287. <https://doi.org/10.1016/j.heliyon.2022.e11287>
- Persons, BS, 1995. *Laterite: Genesis, Location, Use*, 1st edition. ed. Springer US, Boston, MA. <https://doi.org/10.1007/978-1-4684-7215-8>
- Rimbarngaye, A., Mwero, JN, Ronoh, EK, 2022. Effect of gum Arabic content on maximum dry density and optimum moisture content of laterite soil. *Heliyon* 8, e11553. <https://doi.org/10.1016/j.heliyon.2022.e11553>
- Natural Risks, B., 2020. Characterization of blocks produced by the addition of coconut fibers and laterite-cement-based building materials. *Africa Science* 17, 170–184.
- Ristić, M., Musić, S., Godec, M., 2006. Properties of γ -FeOOH, α -FeOOH and α -Fe₂O₃ particles precipitated by hydrolysis of Fe³⁺ ions in perchlorate containing aqueous solutions. *Journal of Alloys and Compounds* 417, 292–299. <https://doi.org/10.1016/j.jallcom.2005.09.043>
- Riza, FV, Rahman, IA, Mujahid, A., Zaidi, A., 2010. A brief review of Compressed Stabilized Earth Brick (CSEB), in: 2010 International Conference on Science and Social Research (CSSR 2010). Presented at the 2010 International Conference on Science and Social Research (CSSR), IEEE, Kuala Lumpur, Malaysia, pp. 999–1004. <https://doi.org/10.1109/CSSR.2010.5773936>
- Sanou, A., Coulibaly, M., N'dri, SR, Tămaş, TL, Bizo, L., Frentiu, T., Covaci, E., Abro, KDM, Dablé, PJ-MR, Yao, KB, Fort, CI, Turdean, GL, 2024. Raw clay material-based modified carbon paste electrodes for sensitive heavy metal detection in drinking water. *J Mater Sci* 59, 13961–13977. <https://doi.org/10.1007/s10853-024-09945-2>
- Sanou, I., 2017. Influence of the cement-pozzolan mixture on some physical and mechanical properties of adobes (Doctoral Thesis). Ouaga I University Pr Joseph KI-ZERBO, Burkina Faso.
- Sanou, Y., Balogoun, CK, Tiendrebeogo, R., Kabore, R., Tchakala, I., Pare, S., 2020. Physico-chemical and spectroscopic properties of two laterite soils for applications in arsenic water treatment. *Int. J. Multidiscip. Res. Dev.* 7, 12–17.
- Santha Kumar, G., Saini, PK, Deoliya, R., Mishra, AK, Negi, SK, 2022. Characterization of laterite soil and its use in construction applications: A review. *Resources, Conservation & Recycling Advances* 16, 200120. <https://doi.org/10.1016/j.rcradv.2022.200120>
- Schellmann, W., 2003. Discussion of "A critique of the Schellmann definition and classification of laterite" by RP Bourman and CD Ollier (*Catena* 47, 117-131). *Catena* 52, 77–79.
- Setiawan, R., Santosa, W., Sjafruddin, A., 2015. Effect of Habit and Car Access on Student Behavior Using Cars for Traveling to Campus. *Procedia Engineering* 125, 571–578. <https://doi.org/10.1016/j.proeng.2015.11.063>
- Soro, SB, Coulibaly, M., Paul Gauty, L., N'Dri, SR, Sanou, A., Trokourey, A., 2023. Characterization of Clay Materials from Côte d'Ivoire: Possible Application for the Electrochemical Analysis. *JMSR* 12, 51–64. <https://doi.org/10.5539/jmsr.v12n1p51>
- Suzuki, T., Nakamura, A., Niinae, M., Nakata, H., Fujii, H., Tasaka, Y., 2013. Lead immobilization in artificially contaminated kaolinite using magnesium oxide-based materials: Immobilization mechanisms

and long-term evaluation. *Chemical Engineering Journal* 232, 380–387.
<https://doi.org/10.1016/j.cej.2013.07.121>

Taïpabé, D., Doko, KV, Datchossa, TA, Bozabé, RK, Gibigaye, M., 2025. Physic Mechanical Behaviors of Raw Earth Bricks: Case of Laterite Stabilized with Gum Arabic and Reinforced with Sugarcane Bagasse in Chad. *OJCE* 15, 56–69. <https://doi.org/10.4236/ojce.2025.151004>

Taypondou Darman, J., Keyangue Tchouata, JH, Ngôn Ngôn, GF, Ngapgue, F., Lindou Ngakoupain, B., Tchedele Langollo, Y., 2022. Evaluation of lateritic soils of Mbé for use as compressed earth bricks (CEB). *Heliyon* 8, e10147. <https://doi.org/10.1016/j.heliyon.2022.e10147>

Walker, PJ, 1995. Strength, durability and shrinkage characteristics of cement stabilized soil blocks. *Cement and Concrete Composites* 17, 301–310. [https://doi.org/10.1016/0958-9465\(95\)00019-9](https://doi.org/10.1016/0958-9465(95)00019-9)

Yvon, J., Liétard, O., Cases, J.-M., Delon, J.-F., 1982. Mineralogy of kaolinic clays from the Charentes. *bulmi* 105, 431–437. <https://doi.org/10.3406/bulmi.1982.7565>

Zolfaghari, Z., Mosaddeghi, MR, Ayoubi, S., Kelishadi, H., 2015. Soil atterberg limits and consistency indices as influenced by land use and slope position in Western Iran. *J.Mt.Sci.* 12, 1471–1483.
<https://doi.org/10.1007/s11629-014-3339-z>

(2025) ; <http://www.jmaterenvironsci.com>